CERN - EUROPEAN ORGANIZATION FOR NUCLEAR RESEARCH

Submitted to
Physics Letters B

CERN/EP/PHYS 77-8
3 March 1977

THE K^-p CHARGE EXCHANGE AND ELASTIC SCATTERING REACTIONS AT 4.2 GeV/c

Amsterdam-CERN-Nijmegen-Oxford Collaboration

F. MARZANO(*), D.Z. TOET(**), Ph. GAVILLET, J.B. GAY(***), R.J. HEMINGWAY and B. MARECHAL(+)
CERN, European Organization for Nuclear Research, Geneva, Switzerland.

R. BLOKZIJL, B. JONGEJANS, J.C. KLUYVER and G.F. WOLTERS
Zeeman Laboratorium, Universiteit van Amsterdam, Amsterdam, Netherlands(++).

P.M. HEINEN and D.J. SCHOTANUS
University of Nijmegen, Nijmegen, Netherlands(++).

P. GROSSMANN and J. WELLS
Nuclear Physics Laboratory, Oxford University, Oxford, U.K.

ABSTRACT

In this letter results are presented on the reactions $K^-p \to \bar{K}^on$ and $K^-p \to K^-p$ from a high statistics CERN 2-metre hydrogen bubble chamber exposure at 4.15 GeV/c. The behaviour of the differential cross section as a function of four-momentum transfer shows remarkable similarities between the two reactions studied. From a comparison of our data with K^+p elastic scattering at 4.27 GeV/c we draw some conclusions concerning the magnitude of the contributing amplitudes.

(*) CERN Fellow from INFN, Sezione di Roma.

(**) Now at NIKHEF (Dutch National Institute for Nuclear Physics and High Energy Physics), sect. H, Amsterdam.

(***) Now at Ecole Polytechnique Fédérale, Lausanne.

(+) Now at Dept. de Fisica, Universidade de Brasilia.

(++) This investigation was supported by the joint research programs of F.O.M. and Z.W.O.

RJH/ed

The data for the reactions

$$K^- p \to \overline{K^o} n \quad (1)$$

and $$K^- p \to K^- p \quad (2)$$

reported on in this paper essentially cover the full production angular range. Only the data for reaction (2) in the region $|t| < 0.1$ GeV^2 is not used because it suffers from scanning and processing losses and would require large correction factors. The statistical level is $\sim$ 80 events/μb for reaction (1), and $\sim$ 5 events/μb for reaction (2), which was measured in a limited sample of film. Both samples however have a comparable overall statistical significance because the total cross section for reaction (2) is approximately 17 times larger than for reaction (1). Results from both reactions obtained in an early stage of the experiment have been previously published [1, 2]. The data of ref. [1] is included in the present sample, that of ref. [2] is not because it was obtained from part of the statistics by a special scan concentrating on the small $|t|$-region.

The events found at the scanning stage were measured either on conventional film-plane digitisers or semi-automatic measuring devices. The measurements were processed via the CERN geometry and kinematics programmes. In case of multiple kinematic interpretations events were investigated on the scanning table if the predicted ionizations allowed visual discrimination. Failing events were remeasured. After two measurements approximately 5% of the events expected to belong to the channels studied were left without a kinematic fit.

To study reaction (1) we selected events of the type zero-prong plus associated V^o-decay. Approximately 4% of these events - predominantly associated with a fast V^o - have an ambiguous (K^o/Λ) interpretation. They show up as a spike in the distribution of the cosine of the angle ϕ between the positive decay track and the V^o direction in the V^o rest frame (which is expected to be flat) in the region when $0.80 < \cos\phi < 0.95$. By removing all events in this region and weighting the remainder we have eliminated all K^o/Λ ambiguities in an unbiased way. For the remaining 48 532 events, fig. 1 shows the distribution of the effective mass recoiling against the K^o. A clear neutron signal is visible. We defined our sample of charge exchange events by selecting the fits with a probability > 2% and applying cuts on the fiducial volume, the beam momentum and the projected decay length (3 mm). The final sample contains 5412 events. To compensate for cuts and losses weights were assigned where appropriate. The average value of this weight amounts to 1.3. The total charge exchange cross section for the average beam momentum of 4.15 GeV/c was determined to be 266 ± 11 μb. The 4% error contains a 1.5% statistical and a 2.5% systematic contribution reflecting the uncertainty in absolute normalization.

An investigation of the events which did not fit after two measurements - amounting to 5% of the sample - did not show appreciable bias in the differential cross section.

The differential cross section for reaction (1) is presented in fig. 2 and table 1(*). It shows a clear turnover in the forward region ($0. < |t|$ (GeV^2) < 0.1) and can be approximately described by an exponential in the regions $0.08 < |t|$ (GeV)^2 $< .6$ and $1.2 < |t|$ (GeV)^2 < 6. By fitting an expression of the form $d\sigma/dt \sim \exp(-A|t|)$ to the experimental differential cross section in these $|t|$ intervals we determined the slope parameters A quoted in table 2. The intermediate region $.6 < |t|$ (GeV^2) < 1.2 shows a break at $|t| \sim 0.6$ GeV^2, followed by a dip at $|t| \sim 1.$ GeV^2 and a secondary maximum near $|t| \sim 1.2$ GeV^2. There is no evidence for backward production: no events were found above $|t| \sim 6$ GeV^2, which leads to an upper limit of 0.12 μb (at 90% confidence level) for the cross section between $|t| = 6.0$ GeV^2 and $|t|_{max} = 6.76$ GeV^2.

For reaction (2), all events giving a successful kinematic fit to the 4C elastic hypothesis were accepted except for some 800 events that were removed from the sample for reasons of having a beam momentum too far off from the central value. This leaves us with 13 433 events in the full

---

(*) Because of the small difference in mass between the incoming and the produced meson (baryon) in reaction (1) we use $|t|$ instead of t'.

t-range. However, in the region of small momentum transfers ($|t| < 0.1$ GeV^2) the data is strongly affected by scanning/processing inefficiencies due to recoil protons with small projected lengths and steeply dipping tracks. For this reason we use data with $|t| > 0.1$ GeV^2 only. Also for the latter sample an investigation of the distribution of the angle between the scattering plane normal and the direction of the camera optical axes indicated the need for a residual t-dependent correction factor taking account of the losses occuring in the regions around $\pm \pi/2$. This correction amounts to 35% in the $|t|$-interval between 0.10 and 0.12 GeV^2, vanishes around $|t| = 0.4$ GeV^2 and has an average value of 9%.

Events showing a decay of the secondary K^- were not used for this analysis. Because of the long lifetime of the kaon this sample represents only a small fraction of the total elastic event sample produced. Possible biases due to these events were looked for in a sample of elastic kink events originating from the entire exposure and were found to be absent in the t-region studied. In particular, we did not find any such events above $|t| = 3$ GeV^2.

By fitting an expression of the form

$$(dN/dt)_t = (dN/dt)_o \exp(-A|t|)$$

to the corrected event distribution in the $|t|$ interval between 0.14 and 0.6 GeV^2 we determined the slope of the forward differential cross section and the extrapolated value of dN/dt at t = 0.

The normalization factor was derived from the value of the elastic differential cross section at t = 0 GeV^2, obtained through application of the optical theorem which leads to

$$(d\sigma/dt)_{t=0,\ \mathrm{elastic}} = \frac{\sigma_T^2(1+\gamma^2)}{16\pi\alpha^2} \quad ,$$

with

$$\sigma_T = 25.26 \pm 0.40 \text{ mb}$$

$$\gamma = \left[\frac{\mathrm{Re}F^{el}}{\mathrm{Im}F^{el}}\right]_{t=0} = 0.10 \pm 0.04 \text{ [3]} \quad ,$$

where F^{el} denotes the elastic scattering amplitude, and

$$\alpha = 0.624 \text{ GeV. mb}^{\frac{1}{2}} \quad .$$

The value of the total K^-p cross section (σ_T) used in the above expression was estimated on the basis of a fit with a second order polynomial to the values found by other experiments in the beam momentum interval between 2.5 and 6.0 GeV/c [4].

The results for the slope parameter and $(d\sigma/dt)_{t=0}$ are given in table 2.

The differential cross section and event distribution as a function of $|t|$ are given in table 1 while the former is also displayed in fig. 2. The errors quoted are of a statistical nature only. The uncertainty in absolute normalization is estimated to be 4.5%. Qualitatively, also in the high $|t|$-region ($1.5 < |t|$ GeV$^2 < 4.0$) the behaviour is well accounted for by a simple exponential decrease.

The result of a fit, analogous to the one discribed above, in this $|t|$-region is also presented in table 2. The similarity of the slopes for the two reactions in the high $|t|$-region is remarkable. In the intermediate $|t|$-range we find a slight decrease of the slope at $|t| = 0.6$ GeV^2, which is also observed in reaction (1), followed by a dip at $|t| \simeq 0.9$ GeV^2 and a secondary maximum near $|t| = 1.1$ GeV^2. We find no evidence for backward peaking - no events were observed between $|t|$-values of ~ 5 GeV^2 and the maximal value ~ 6.76 GeV^2. This leads to an estimated upper limit (at 90% confidence level) of 0.48 μb for the partial cross section in this t-region. Our backward hemisphere cross section, $\sigma_B = 0.85 \pm 0.43$ μb corresponding to four events, is in agreement with what would be expected on the basis of results from other experiments in the beam momentum range between 2 and 10 GeV/c.

By integrating the differential cross section we obtain a total elastic scattering cross section σ_{el} = 4.50 ± 0.24 mb, the 5.5% error containing the 4.5% systematic contribution due to normalization uncertainties.

The structures in the differential cross section distributions for both the elastic and the charge-exchange (CEX) process (fig. 2) can be understood in terms of the Dual Absorption Model (DAM) [5].

In the CEX case the turnover in the forward direction indicates a significant contribution from the helicity-flip amplitude. The structure around $|t| \sim 1.0$ GeV^2 (and possibly also the one at ~ 0.6 GeV^2) could be related to zero's in both the flip and the non-flip part of the relevant (A_2-ρ) amplitude.

The situation in the elastic channel is more complicated as more exchange amplitudes contribute here and combine in a non-trivial way to produce the observed t-dependence. Nevertheless, the general shape and the dip at $|t| \sim 1.0$ GeV^2 are predicted by the model. As far as the high $|t|$-region is concerned ($|t| > 1.5$ GeV^2), we can only remark that on the basis of the data these amplitudes produce the same dependence on $|t|$ as the (A_2-ρ) amplitude does in the CEX case.

Comparing our elastic differential cross section to that of $K^+p \to K^+p$ obtained by Seidl [6] in a bubble chamber experiment at approximately the same momentum (4.27 GeV/c) one obtains a first crossover at $|t|$ = 0.225 ± 0.010 GeV^2, in agreement with the result of Brandenburg et al. [7] (0.219 ± 0.007 GeV^2) at 6.4 GeV/c, but somewhat higher than the value obtained by Ambats et al. [8] (0.189 ± 0.007 GeV^2) at 3.65 and 5.0 GeV/c K momentum.

As pointed out by Davier and Harari [9], a comparison of K^+p and K^-p elastic scattering at the same energy can, under the assumptions of the dual absorptive model, yield information on the imaginary part of the non-diffractive non-flip contribution to the elastic scattering amplitude

$F^{el}_{\Delta\lambda = 0}$ via the relation

$$\mathrm{Im}F^{el}_{\Delta\lambda = 0} = \frac{d\sigma/dt\ (K^-p) - d\sigma/dt\ (K^+p)}{2(d\sigma/dt\ (K^+p))^{\frac{1}{2}}} \quad . \tag{3}$$

The behaviour of $\mathrm{Im}F_{\Delta\lambda = 0}$ as a function of $|t|$ is predicted to be described by an expression of the form

$$\mathrm{Im}F^{el}_{\Delta\lambda = 0} = A \exp (Bt)\ J_o\ (C\sqrt{-t}) \quad .$$

By using K^+p elastic scattering data at 4.27 GeV/c [6], we are in a position to make a straightforward comparison at almost equal energies without the need for interpolation. We fitted the above expression to the experimental data in the interval $0.1 < |t|\ (\mathrm{GeV}^2) < 2.0$. The resulting parameter values are: $A = 1.87 \pm 0.14\ \mathrm{mb}^{\frac{1}{2}}\ \mathrm{GeV}^{-1}$, $B = 1.04 \pm 0.11\ \mathrm{GeV}^{-2}$ and $C = 4.956 \pm 0.039\ \mathrm{GeV}^{-1} = 0.978 \pm 0.008$ Fermi ($\chi^2/\mathrm{NDF} = 31/22$), which indicates dominance of a partial wave with $J = pC = 13/2$ (p = c.m. momentum) in agreement with the results quoted in ref. [6]. For a discussion of some complications we refer to ref. [10]

Writing expression (3) in terms of Regge exchanges and substituting the values of the differential cross section at $t = 0\ \mathrm{GeV}^2$ for the elastic process studied in our experiment, and that published in ref. [6] respectively we get (at $t = 0\ \mathrm{GeV}^2$)

$$\mathrm{Im}F^{el}_{\Delta\lambda = 0} = 2\ \mathrm{Im}(\omega + \rho^{el})_{\Delta\lambda = 0} = 1.94 \pm 0.31\ \mathrm{mb}^{\frac{1}{2}}/\mathrm{GeV} \ . \tag{4}$$

Expressing now the CEX differential cross section in terms of helicity flip and non-flip amplitudes

$$\frac{d\sigma}{dt}(\mathrm{CEX}) = |F^{CEX}_{\Delta\lambda = 0}|^2 + |F^{CEX}_{\Delta\lambda = 1}|^2$$

and using the small θ^* - (or small t) - approximation $F^{CEX}_{\Delta\lambda} \approx (\sin \frac{\theta^*}{2})^{\Delta\lambda}$ (where θ^* denotes the c.m.s scattering angle), we can extract from our data the magnitude of the non-flip amplitude at $t = 0\ \mathrm{GeV}^2$

$$|F^{CEX}_{\Delta\lambda\ =\ 0}| = \frac{d\sigma}{dt}(t = 0)^{\frac{1}{2}} = |(A_2 - \rho)^{CEX}| = 0.66 \pm 0.04\ \mathrm{mb}^{\frac{1}{2}}/\mathrm{GeV} \tag{5}$$

Using the general Dual Absorption Model assumptions [5] and exchange degeneracy (EXD)

$$\mathrm{Re}\ \rho = \mathrm{Im}\ \rho;\ \mathrm{Re}\ A_2 = -\ \mathrm{Im}\ A_2;\ \mathrm{Im}\ A_2 = -\mathrm{Im}\ \rho.$$

We obtain from (5), also applying isospin relations

$$\mathrm{Im}\ \rho^{CEX} = -\mathrm{Im}\ A_2^{CEX} = 2\ \mathrm{Im}\ \rho^{e\ell} = 0.33 \pm 0.02\ \mathrm{mb}^{\frac{1}{2}}/\mathrm{GeV}\ \text{at}\ t = 0\ \mathrm{GeV}^2.$$

From (4) we then calculate

$$\mathrm{Im}\ \omega = 0.80 \pm 0.16\ \mathrm{mb}^{\frac{1}{2}}/\mathrm{GeV}\ \text{at}\ t = 0\ \mathrm{GeV}^2,$$

which shows that in elastic scattering the ω-amplitude dominates the ρ-amplitude at $t = 0\ \mathrm{GeV}^2$ by a factor ~ 5 in magnitude. This result is compatible with that reviewed in ref. [5].

We are indebted to the scanning and measuring staffs of the collaborating laboratories and the operating crews of the CERN proton synchrotron and the CERN 2-metre hydrogen bubble chamber.

$F^{el}_{\Delta\lambda = 0}$ via the relation

$$\mathrm{Im}F^{el}_{\Delta\lambda = 0} = \frac{d\sigma/dt\ (K^-p) - d\sigma/dt\ (K^+p)}{2(d\sigma/dt\ (K^+p))^{\frac{1}{2}}} \quad . \tag{3}$$

The behaviour of $\mathrm{Im}F_{\Delta\lambda = 0}$ as a function of $|t|$ is predicted to be described by an expression of the form

$$\mathrm{Im}F^{el}_{\Delta\lambda = 0} = A \exp (Bt)\ J_o\ (C\sqrt{-t}) \quad .$$

By using K^+p elastic scattering data at 4.27 GeV/c [6], we are in a position to make a straightforward comparison at almost equal energies without the need for interpolation. We fitted the above expression to the experimental data in the interval $0.1 < |t|\ (\mathrm{GeV}^2) < 2.0$. The resulting parameter values are: $A = 1.87 \pm 0.14\ \mathrm{mb}^{\frac{1}{2}}\ \mathrm{GeV}^{-1}$, $B = 1.04 \pm 0.11\ \mathrm{GeV}^{-2}$ and $C = 4.956 \pm 0.039\ \mathrm{GeV}^{-1} = 0.978 \pm 0.008$ Fermi ($\chi^2/\mathrm{NDF} = 31/22$), which indicates dominance of a partial wave with $J = pC = 13/2$ (p = c.m. momentum) in agreement with the results quoted in ref. [6]. For a discussion of some complications we refer to ref. [10]

Writing expression (3) in terms of Regge exchanges and substituting the values of the differential cross section at $t = 0\ \mathrm{GeV}^2$ for the elastic process studied in our experiment, and that published in ref. [6] respectively we get (at $t = 0\ \mathrm{GeV}^2$)

$$\mathrm{Im}F^{el}_{\Delta\lambda = 0} = 2\ \mathrm{Im}(\omega + \rho^{el})_{\Delta\lambda = 0} = 1.94 \pm 0.31\ \mathrm{mb}^{\frac{1}{2}}/\mathrm{GeV} \ . \tag{4}$$

Expressing now the CEX differential cross section in terms of helicity flip and non-flip amplitudes

$$\frac{d\sigma}{dt}(\mathrm{CEX}) = |F^{CEX}_{\Delta\lambda = 0}|^2 + |F^{CEX}_{\Delta\lambda = 1}|^2$$

and using the small θ^* - (or small t) - approximation $F^{CEX}_{\Delta\lambda} \approx (\sin \frac{\theta^*}{2})^{\Delta\lambda}$ (where θ^* denotes the c.m.s scattering angle), we can extract from our data the magnitude of the non-flip amplitude at $t = 0\ \mathrm{GeV}^2$

$$|F^{CEX}_{\Delta\lambda = 0}| = \frac{d\sigma}{dt}(t = 0)^{\frac{1}{2}} = |(A_2 - \rho)^{CEX}| = 0.66 \pm 0.04 \text{ mb}^{\frac{1}{2}}/\text{GeV} \qquad (5)$$

Using the general Dual Absorption Model assumptions [5] and exchange degeneracy (EXD)

$$\text{Re } \rho = \text{Im } \rho; \text{ Re } A_2 = - \text{Im } A_2; \text{ Im } A_2 = -\text{Im } \rho.$$

We obtain from (5), also applying isospin relations

$$\text{Im } \rho^{CEX} = -\text{Im } A_2^{CEX} = 2 \text{ Im } \rho^{e\ell} = 0.33 \pm 0.02 \text{ mb}^{\frac{1}{2}}/\text{GeV at } t = 0 \text{ GeV}^2.$$

From (4) we then calculate

$$\text{Im } \omega = 0.80 \pm 0.16 \text{ mb}^{\frac{1}{2}}/\text{GeV at } t = 0 \text{ GeV}^2,$$

which shows that in elastic scattering the ω-amplitude dominates the ρ-amplitude at $t = 0$ GeV^2 by a factor ~ 5 in magnitude. This result is compatible with that reviewed in ref. [5].

We are indebted to the scanning and measuring staffs of the collaborating laboratories and the operating crews of the CERN proton synchrotron and the CERN 2-metre hydrogen bubble chamber.

REFERENCES

[1] R. Blokzijl et al., Nucl. Phys. B51 (1973) 535.

[2] Th.H.J. Bellm et al., Phys. Letters 33B (1970) 438.

[3] P. Baillon et al., Nucl. Phys. B107 (1976) 189.

[4] HERA-Group Compilation, CERN/HERA 72-2.

[5] For a recent review see G.L. Kane and A. Seidl, Rev. Mod. Phys. 48 (1976) 309.

[6] A. Seidl, Phys. Rev. D7 (1973) 621.

[7] G. Brandenburg et al., Phys. Letters 58B (1975) 367.

[8] J. Ambats et al., Phys. Rev. 9D (1974) 1179.

[9] M. Davier and H. Harari, Phys. Letters 35B (1971) 239.

[10] R. Carnegie et al., Phys. Letters 58B (1975) 371.

TABLE CAPTIONS

Table 1 Values of the differential cross sections and numbers of observed events as a function of four-momentum transfer squared for the reactions $K^-p \rightarrow K^-p$ and $K^-p \rightarrow \bar{K}^0n$ at 4.2 GeV/c.

Table 2 Fitted slope parameters for the differential cross sections of the reactions $K^-p \rightarrow \bar{K}^0n$ and $K^-p \rightarrow K^-p$ at 4.2 GeV/c. The value of $(d\sigma/dt)_{t=0}$ for the latter reaction was calculated from the optical theorem.

TABLE 1

|t|-interval GeV^2		$K^-p \to K^-p$ $\frac{d\sigma}{dt} \pm \Delta\left(\frac{d\sigma}{dt}\right)$ μb GeV^{-2}	$K^-p \to K^-p$ No of observed events	$K^-p \to \overline{K^o}n$ $\frac{d\sigma}{dt} \pm \Delta\left(\frac{d\sigma}{dt}\right)$ μb GeV^{-2}	$K^-p \to \overline{K^o}n$ No of observed events
.00	.02			488 ± 35	198
.02	.04			575 ± 42	229
.04	.06			664 ± 41	265
.06	.08			619 ± 40	247
.08	.10			619 ± 38	255
.10	.12	14,530 ± 490	1066	578 ± 37	236
.12	.14	12,520 ± 430	1063	567 ± 38	233
.14	.16	10,860 ± 530	937	511 ± 37	207
.16	.18	9,260 ± 470	825	483 ± 35	190
.18	.20	7,790 ± 410	707	475 ± 35	194
.20	.22	6,930 ± 340	638	444 ± 33	185
.22	.24	6,000 ± 310	557	412 ± 31	168
.24	.26	5,450 ± 290	509	402 ± 34	164
.26	.28	4,390 ± 250	412	379 ± 30	150
.28	.30	3,600 ± 210	339	320 ± 28	133
.30	.35	2,970 ± 130	701	321 ± 16	322
.35	.40	2,030 ± 100	483	242 ± 14	244
.40	.45	1,430 ± 77	345	187 ± 13	189
.45	.50	873 ± 60	211	164 ± 12	166
.50	.55	703 ± 54	170	137 ± 11	145
.55	.60	468 ± 44	113	114 ± 9.0	114
.60	.65	277 ± 34	67	80.0 ± 8.9	81
.65	.70	240 ± 32	58	77.6 ± 8.4	80
.70	.75	207 ± 29	50	72.0 ± 7.6	75
.75	.80	157 ± 26	38	59.3 ± 8.0	62
.80	.85	91 ± 19	22	62.1 ± 7.2	63
.85	.90	66 ± 17	16	50.9 ± 7.7	51
.90	.95	124 ± 23	30	52.9 ± 7.2	51
.95	1.00	83 ± 19	20	41.2 ± 5.8	37
1.00	1.10	112 ± 15	54	30.8 ± 3.9	65
1.10	1.20	101 ± 15	49	35.4 ± 3.9	73
1.20	1.30	73 ± 12	35	32.3 ± 4.3	67
1.30	1.40	85 ± 13	41	31.1 ± 3.7	64
1.40	1.50	41.2 ± 9.2	20	28.1 ± 3.5	54
1.50	1.75	36.2 ± 5.5	44	22.8 ± 2.1	119
1.75	2.00	23.0 ± 4.4	28	14.8 ± 1.8	76
2.00	2.25	14.8 ± 3.5	18	10.2 ± 1.4	51
2.25	2.50	9.1 ± 2.7	11	7.2 ± 1.0	36
2.50	2.75	10.8 ± 3.0	13	4.0 ± 1.0	20
2.75	3.00	5.0 ± 2.0	6	2.4 ± .6	12
3.00	3.50	2.5 ± 1.4	3	2.2 ± .4	23
3.50	4.00	1.2 ± .7	3	.24 ± .1	2
4.00	5.00	.2 ± .2	1	.19 ± .12	4
5.00	6.00	0. ± 0.	o	.09 ± .06	2

TABLE 2

Reaction	$\|t\|$-region GeV^2	slope A GeV^{-2}	$d\sigma/dt$ (t = 0) mb GeV^{-2}
$K^- p \rightarrow \overline{K^o} n$	.08 - .6	3.51 ± .12	-
	1.2 - 6.0	1.66 ± .07	-
$K^- p \rightarrow K^- p$	0.14 - 0.60	7.44 ± 0.11	32.9 ± 1.1
	1.50 - 4.00	1.60 ± 0.17	-

FIGURE CAPTIONS

Fig. 1 Distribution of the effective mass recoiling against the K^o.

Fig. 2 Differential cross sections of the reactions $K^-p \rightarrow K^-p$ and $K^-p \rightarrow \overline{K^o}n$ as a function of $|t|$.

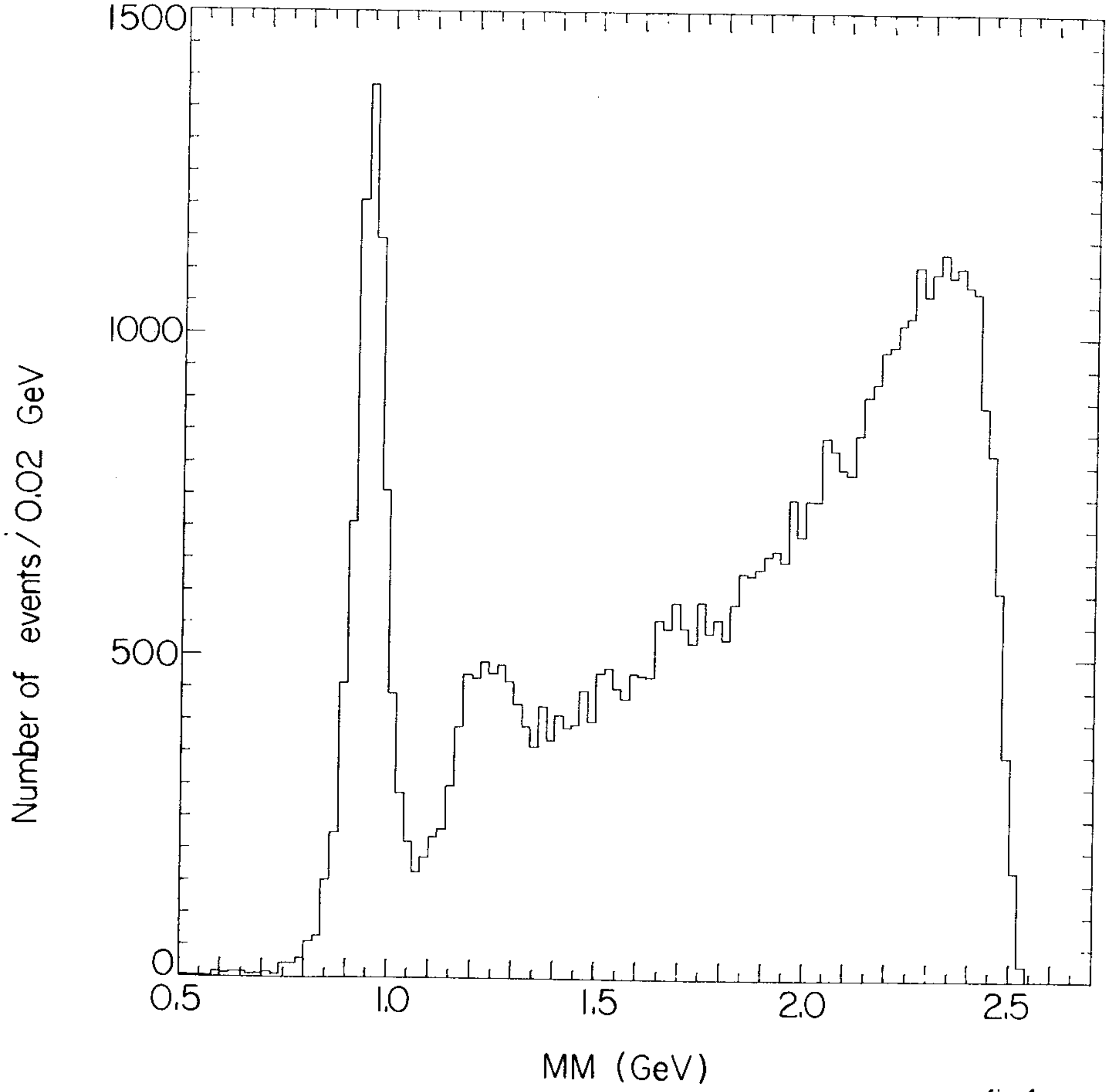

fig.1

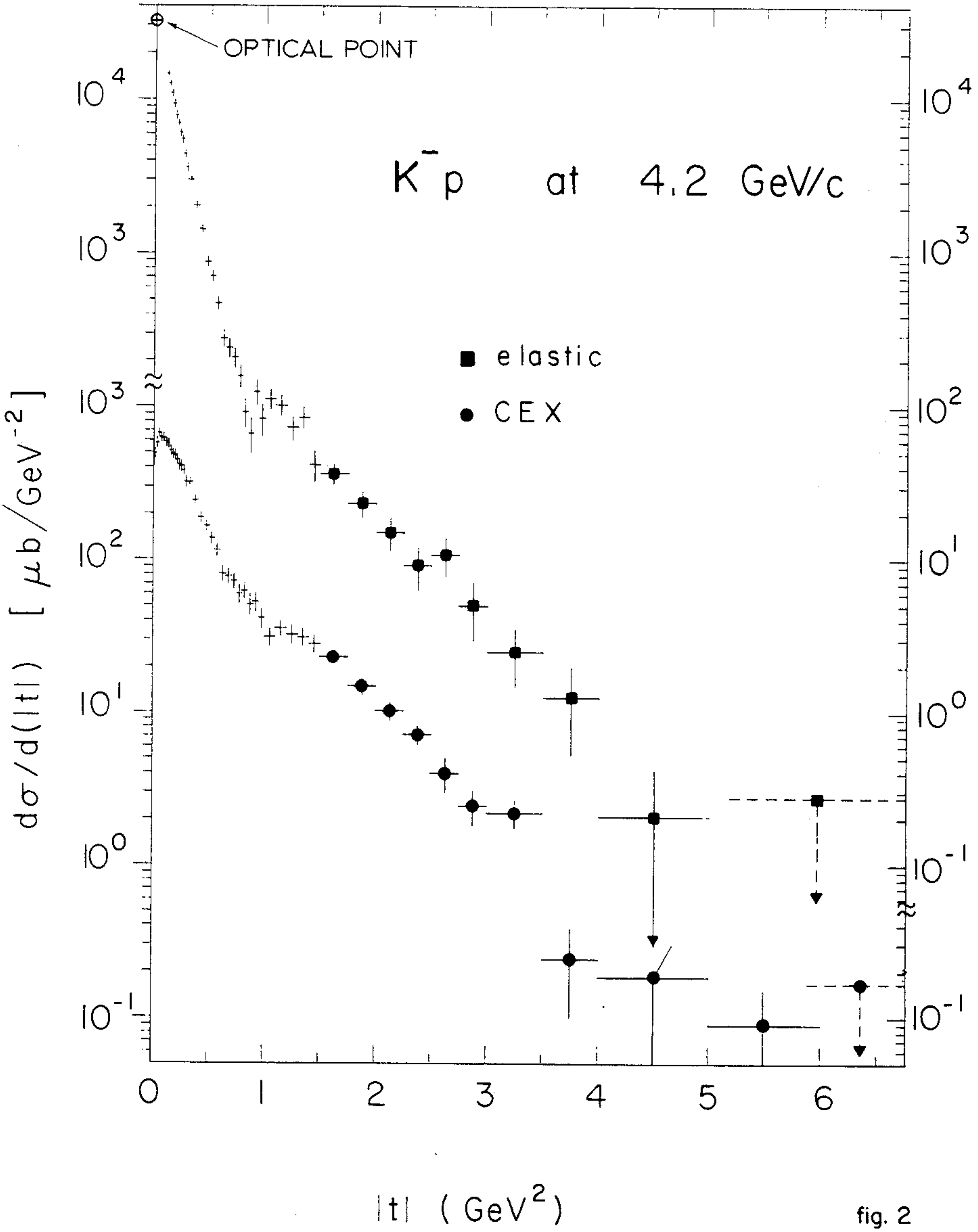

fig. 2